iScience

Article

Effects of aging on diurnal transcriptome change in the mouse corpus callosum

Graphical abstract

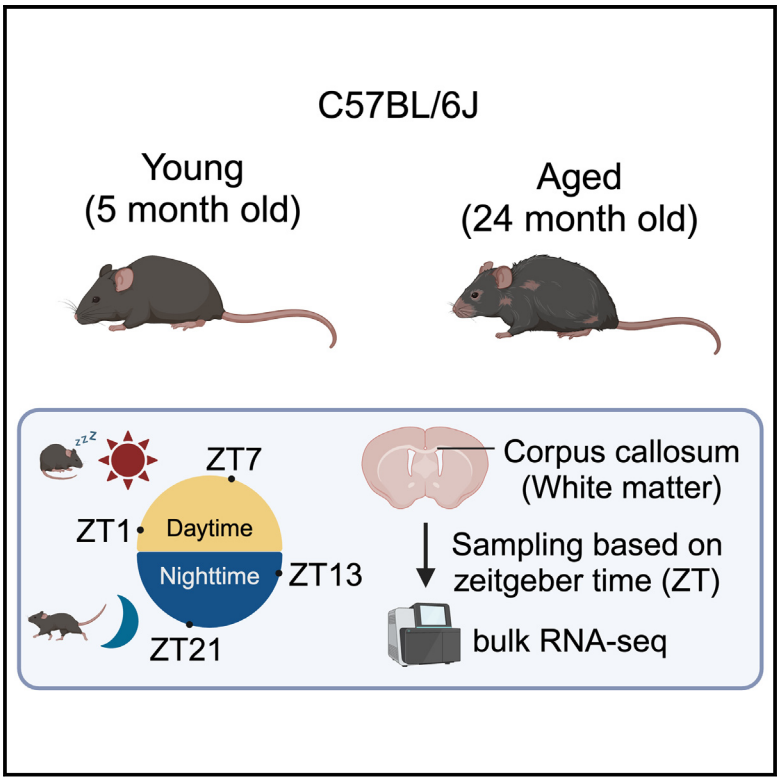

Highlights

- RNA-seq was performed on the corpus callosum of young and aged mice at four time points
- Aging alters time-dependent gene expression patterns in the corpus callosum
- Complement pathway genes consistently upregulated in aged mice at all time points

Authors

Hidehiro Ishikawa, Tomonori Hoshino, Gen Hamanaka, ..., Mary E. Harrington, Eng H. Lo, Ken Arai

Correspondence

lo@helix.mgh.harvard.edu (E.H.L.), karai@partners.org (K.A.)

In brief

Age; Neuroscience; Transcriptomics

Ishikawa et al., 2025, iScience *28*, 111556
January 17, 2025
https://doi.org/10.1016/j.isci.2024.111556

CellPress

iScience

CellPress
OPEN ACCESS

Article

Effects of aging on diurnal transcriptome change in the mouse corpus callosum

Hidehiro Ishikawa,[1,2,5] Tomonori Hoshino,[1,5] Gen Hamanaka,[1] Emiri T. Mandeville,[1] Shuzhen Guo,[1] Shintaro Kimura,[1] Norito Fukuda,[1] Wenlu Li,[1] Akihiro Shindo,[2] Sava Sakadzic,[3] Mary E. Harrington,[4] Eng H. Lo,[1,*] and Ken Arai[1,6,*]

[1]Neuroprotection Research Laboratories, Departments of Radiology and Neurology, Massachusetts General Hospital and Harvard Medical School, Charlestown, MA 02129, USA

[2]Department of Neurology, Mie University Graduate School of Medicine, 2-174 Edobashi, Tsu, Mie 514-8507, Japan

[3]Athinoula A. Martinos Center for Biomedical Imaging, Massachusetts General Hospital, Harvard Medical School, Charlestown, MA 02129, USA

[4]Neuroscience Program, Smith College, Northampton, MA 01060, USA

[5]These authors contributed equally

[6]Lead contact

*Correspondence: lo@helix.mgh.harvard.edu (E.H.L.), karai@partners.org (K.A.)

https://doi.org/10.1016/j.isci.2024.111556

SUMMARY

The corpus callosum, a major white matter region central to cognitive function, is vulnerable to aging. Using zeitgeber time (ZT) aligned with environmental light/dark cycles, we investigated temporal gene expression patterns in the corpus callosum of young (5-month-old) and aged (24-month-old) mice using RNA-seq. Comparative analysis revealed more differentially expressed genes across ZT pairs in young mice than aged mice. In addition, complement pathway genes, including *C4b*, *C3*, *C1qa*, *C1qb*, and *C1qc*, were consistently upregulated in aged mice regardless of ZT. Furthermore, genes such as *Etnppl*, *Tinagl1*, *Hspa12b*, *Ppp1r3c*, *Thbd*, *Pla2g3*, and *Tsc22d3* exhibited ZT-dependent rhythmicity in young mice, but their rhythmic patterns were altered with age. This study provides an important dataset of the interplay between aging, diurnal rhythms, and gene expression in the corpus callosum, highlighting potential molecular mechanisms mediating white matter aging. Further investigation is warranted to dissect these gene's specific roles in neurological health during aging.

INTRODUCTION

The corpus callosum, one of the largest white matter structures in the brain connecting the left and right cerebral hemispheres, plays a critical role in cognitive function due to its enrichment in oligodendrocyte precursor cells (OPCs) and oligodendrocytes. Aging, a major risk factor for neurodegenerative diseases associated with dementia and motor disorders, significantly affects the corpus callosum, making it one of the most vulnerable brain regions in age-related neurological disorders, such as stroke, Alzheimer's disease, or vascular dementia.[1] Structural examinations of age-related white matter degeneration suggest disruptions in the normal interactions between brain regions.[2] These disruptions may contribute to cognitive decline during normal aging.[2] Studies using diffusion tensor imaging have revealed disruptions in white matter integrity and reduced correlations within higher-order brain systems that correlate with cognitive deficits in various regions.[3] This evidence underscores the critical role of white matter in age-related cognitive decline.

Circadian/diurnal rhythms have emerged as important players in neurological disease and neuroprotection.[4–9] Recent studies increasingly suggest a link between circadian clocks and the process of normal aging.[10–12] While the central nervous system is regulated by the master circadian clock, the suprachiasmatic nucleus (SCN),[13–16] distinct circadian oscillation of clock gene expression in different regions of the central nervous system, such as the SCN, hippocampus, cerebral cortex, and spinal cord, suggest potential tissue-specific effects.[17] Despite extensive research on circadian gene expression profiles in various organs and cell types, including the liver,[18] cerebral cortex,[19] brain endothelial cells,[20] and OPCs/oligodendrocytes,[21] there remains a gap in studies specifically addressing circadian and diurnal gene expression changes in white matter tissues. Therefore, the present study aims to fill this gap by investigating gene expression profiles in the corpus callosum at different zeitgeber time (ZT) points in both young and aged mice.

RESULTS

Isolation of the corpus callosum from young and aged mice and gene expression profiling using zeitgeber time

zeitgeber time (ZT) is a standardized 24-h notation system used in circadian biology, where ZT0 corresponds to the onset of the light phase, and ZT12 corresponds to the onset of the dark phase in a 12:12 light/dark cycle. For example, ZT1 corresponds to 1 h after lights are turned on in a 12:12 laboratory-controlled

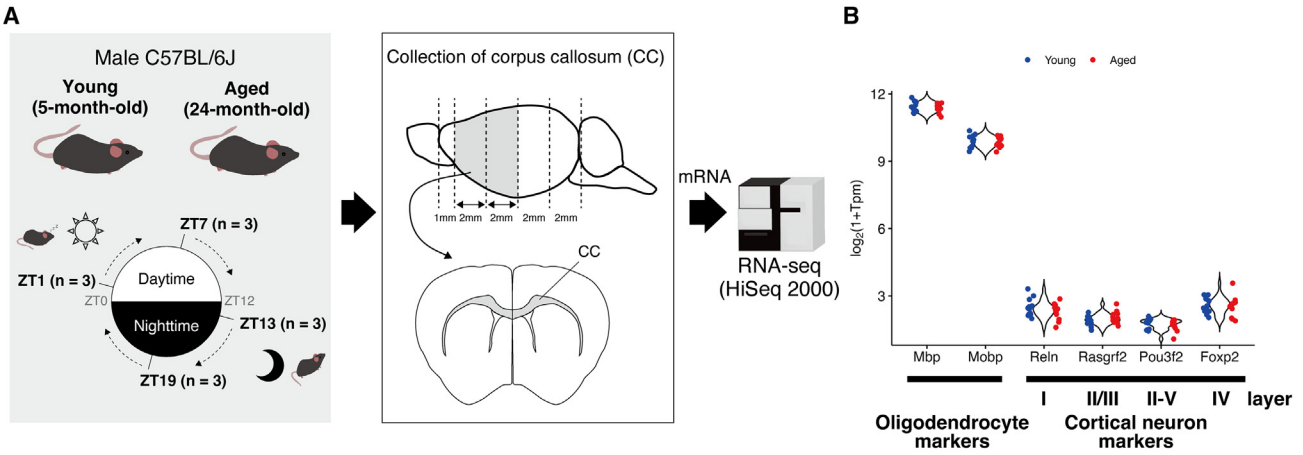

Figure 1. Tissue sampling at specific time points and preparation for RNA-seq analysis

(A) Samples were collected from the anterior part of the corpus callosum (CC) of young (5 months old) and aged (24 months old) mice. The isolated RNA was then used for RNA-seq analysis. Three samples were collected at each of the four ZTs (ZT1/ZT7/ZT13/ZT19) for a total of 24 samples.

(B) Violin plots showing the expression of oligodendrocyte markers (*Mbp* and *Mobp*) and cortical neuron markers (*Reln* for layer I, *Rasgrf2* for layer II/III, *Pou3f2* for layer II-V, and *Foxp2* for layer IV).

environment, while ZT13 corresponds to 1 h after lights are turned off. In this study, we examined gene expression profiles at different ZTs to identify potential temporal patterns using bulk RNA sequencing (RNA-seq). The corpus callosum was collected from young (5 months of age) and aged (24 months of age) male mice at each of the four time points: ZT1, ZT7, ZT13, and ZT19 (Figure 1A). To validate the successful isolation of the corpus callosum, we examined the gene expression of cellular markers for oligodendrocytes and neurons in each cortical layer. This confirmed that the samples were indeed white matter tissue, as evidenced by the high expression of oligodendrocyte markers (Figure 1B).

Analysis of diurnal gene expression patterns in the corpus callosum of young and aged mice

To understand the diurnal regulation of genes in the corpus callosum, we first examined the expression patterns of circadian genes in both young and aged mice (Figure 2A). Our results indicated that *Nr1d1*, *Nr1d2*, *Arntl* (also known as *Bmal1*), *Cry1*, *Per2*, and *Per3* maintained their daily periodicity with ZT in both young and aged mice (Figures 2B and 2C; one-way analysis of variance [ANOVA], $p < 0.05$). In addition, using compareRhythms,[22,23] we confirmed that these genes retained their diurnal patterns across the two groups. However, *Rora*, *Clock*, *Cry2*, and *Per1* did not show a daily rhythm in both young and aged mice (Figure 2C).

We then examined whether the diurnal periodicity of other genes was affected by age. Looking at young mice, as shown in the Venn diagrams and UpSet plots, the number of detected differentially expressed genes (DEGs) was smaller in the ZT1 vs. ZT7 and ZT13 vs. ZT19 pairs, compared to the ZT1 vs. ZT13, ZT1 vs. ZT19, ZT7 vs. ZT13, or ZT7 vs. ZT19 pairs (Figures S1A and S1B). To further investigate whether diurnal patterns are attenuated by aging, we compared DEGs at six-time point pairs (ZT1 vs. ZT7, ZT1 vs. ZT13, ZT1 vs. ZT19, ZT7 vs. ZT13, ZT7 vs. ZT19, and ZT13 vs. ZT19) between young and aged mice (Figure 3A). Young mice exhibited 1, 76, 106, 22, 78, and 36 DEGs at the respective time point pairs, whereas aged mice exhibited 4, 19, 32, 14, 9, and 14 DEGs, respectively (Figure 3B), indicating an overall decrease in ZT-dependent gene expression patterns as mice age. Notably, the total number of DEGs was significantly different, with 200 genes identified in young mice and 70 genes in aged mice, with 20 genes shared between the two groups (Figures 3C and 3D; Table S1).

Transcriptome analysis of the corpus callosum in aging

While the expression levels/patterns of key circadian genes in the corpus callosum were not significantly altered by age (Figure 2), our initial analyses so far suggested age-related changes in the transcriptome profile of the mouse corpus callosum (Figure 3). Therefore, before further investigating age-related changes in diurnal patterns, we performed a time-independent analysis on all samples (Figure 4A; $n = 12$ per group, regardless of ZT) to determine whether aging affects the overall transcriptome profile of the mouse corpus callosum. We identified DEGs (|fold change| > 1.5, adjusted p-value [padj] < 0.05, mean base >50) between young and aged mice, with significantly increased (159 genes) and decreased (46 genes) expression in aged mice compared to young mice (205 DEGs in total) (Figure 4B). To assess whether the inclusion of temporal information would significantly affect the finding, we also performed a Midline Estimating Statistic of Rhythm (MESOR)-based analysis by averaging gene expression across the four ZT points for each group ($n = 3$ per group and per ZT point; Table S2). This MESOR analysis identified 161 DEGs, of which 146 overlapped with the DEGs from the time-independent analysis (Figure S2). This substantial overlap may indicate that the majority of age-related gene expression changes are consistent regardless of temporal consideration.

We next conducted a gene ontology (GO) analysis using the 205 DEGs identified from the time-independent analysis. The GO analysis revealed that several GO terms among the top 10

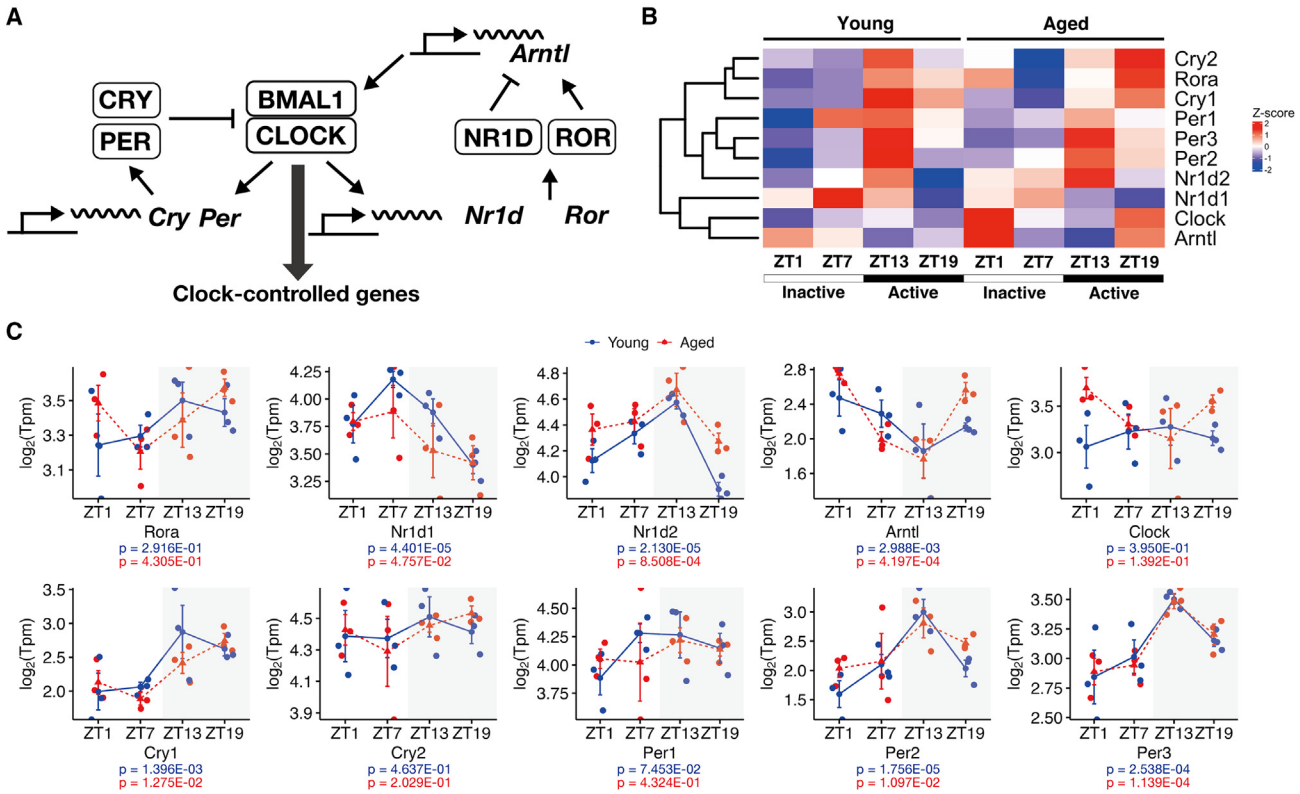

Figure 2. Alterations in circadian rhythm-associated gene expression patterns in the corpus callosum due to aging

(A) Schematic illustration shows the pathways of major circadian rhythm-related genes.

(B) Heatmap showing the various genes associated with diurnal rhythm in the corpus callosum of young and aged mice.

(C) Line plot shows the expression patterns across ZTs for selected circadian rhythm-associated genes in young and aged mice. Data are represented as mean +/− standard error of the mean (SEM). The *p*-values for young mice (blue) and aged mice (red) are derived from one-way ANOVA.

were associated with glial cells and immune responses (Figure 4C). These included microglia pathogen phagocytosis pathway (WP3626), Tyrobp causal network in microglia (WP3625), innate immune response (GO: 0045087), positive regulation of immune response (GO: 0050778), immune effector process (GO: 0002252), and regulation of innate immune response (GO: 0050776) (Figure 4C). We then used public databases of RNA-seq data from brain cells[24,25] to further investigate in which cell types the age-associated DEGs are expressed. The results showed that many of these genes were highly expressed in microglia, oligodendrocyte lineage cells, and astrocytes (Figure 4D). Indeed, a violin plot of glial cell markers showed a tendency for OPC and oligodendrocyte cell markers to decrease with age, while markers for microglia and astrocytes increased (Figure S3).

In addition, the top 10 DEGs that increased with age were *Cd44*, *Serpina3n*, *C3*, *A2m*, *Lgals3bp*, *Cd84*, *Nlrp5-ps*, *Hbb-bs*, *Hba-a2*, and *C4b* (Figures 4B and S4A). Conversely, the top 10 DEGs that decreased with age were *Kif19a*, *Col11a1*, *Tnc*, *Mki67*, *Cacna2d4*, *Mdga1*, *H1f1*, *Gpr17*, *Chst3*, and *Sox11* (Figures 4B and S4B). Since two complement-related genes (*C3* and *C4b*) were included in the top 10 DEGs that increased with age, we investigated the top 5% of genes that showed high expression exclusively in aged mice and confirmed that those genes were highly associated with the complement pathway (Figures S5A and S5B). Furthermore, in addition to *C4b* and *C3*, complement pathway-related factors, such as *C1qa*, *C1qb*, and *C1qc*, showed significant upregulation in aged mice (Figures S5C, and S5D). Among these genes, *C4b*, *C3*, *C1qa*, and *C1qc* were identified as common DEGs at ZT1, ZT7, ZT13, and ZT19 between young and aged mice (Figures S6A and S6B). Furthermore, complement pathway-related genes such as *C3*, *C1qa*, *C1qb*, and *C1qc* showed significant upregulation in aged mice, with no ZT-related changes in expression observed in either young or aged mice (Figure 5). Although *C4b* exhibited a slight rhythm in young mice (one-way ANOVA, p = 2.742E-02), its expression was significantly increased in aged mice regardless of ZT.

Effects of aging on rhythmic gene expression in the corpus callosum

We finally examined how rhythmic gene expression was altered by aging in the mouse corpus callosum. Using one-way ANOVA analysis (threshold: $p < 0.05$), we first identified 1,745 rhythmically expressed genes in young mice and 1,262 rhythmically expressed genes in aged mice (a total of 2,837 genes; Table S3). As expected, GO analysis of the rhythmically expressed genes in young mice ranked a circadian/diurnal rhythm-related term

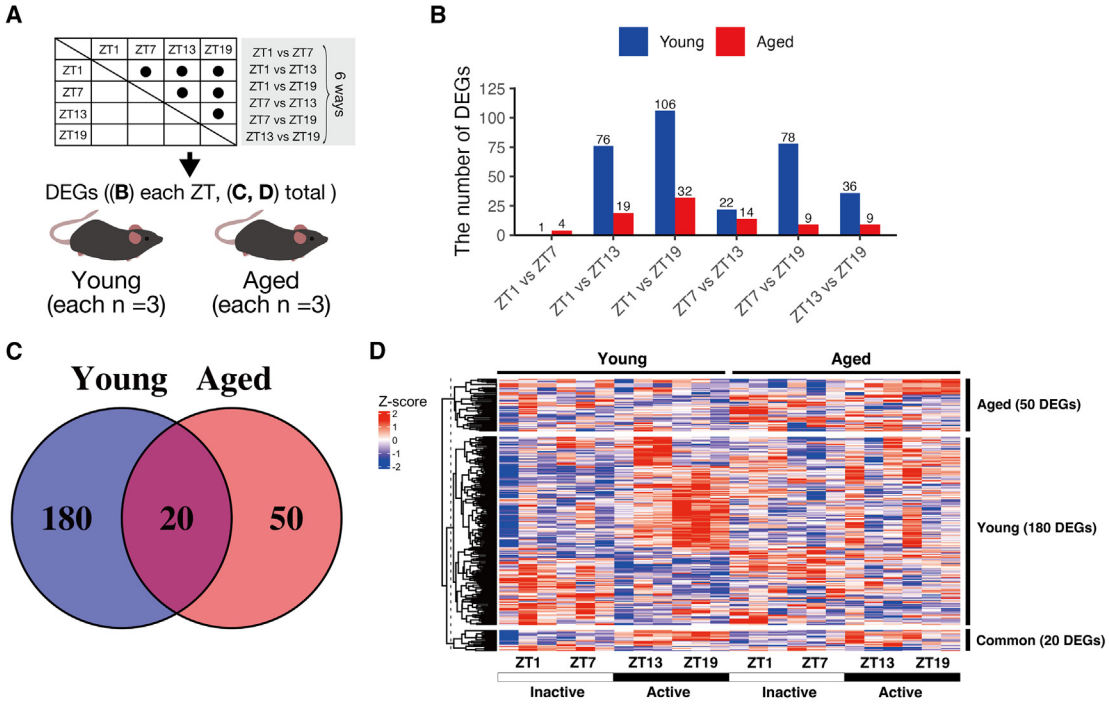

Figure 3. Transcriptome profiling in the corpus callosum using pairwise comparisons among ZTs

(A) Pairwise comparisons among the four ZTs (ZT1, ZT7, ZT13, ZT19) were used to detect DEGs in young and aged mice.

(B) Bar graph shows the number of DEGs identified in each pairwise comparison between ZTs for young and aged mice.

(C) Venn diagram shows the overlap between DEGs from all pairwise comparisons in young and aged mice.

(D) Heatmap of DEGs organized according to the overlapping and non-overlapping regions in (C), showing genes common to both age groups and those unique to either young or aged mice. The cutoff for DEGs was set at adjusted *p*-value (padj) <0.05 and | Fold Change | >1.5.

(mmu04710) among the top 10 highly enriched terms (Figure 6A).

Next, we asked how aging affected these rhythmically expressed genes. Among a total of 2,837 diurnal rhythm genes identified in young and aged mice, we identified 97 genes that showed significant changes in rhythmicity between the two groups (compareRhythms FDR <0.05; Figure 6B). Among these 97 genes, 35 genes were included among the DEGs (padj <0.05) at either ZT1, ZT7, ZT13, or ZT19 in the comparisons between young and aged mice: at ZT1 (*Ddah2*, *Etnppl*, *Col11a1*, *Cdh8*, *Insc*, *C4b*, *Nkain1*, *Gm11611*, and *Rps7-ps3*); at ZT7 (*Col11a1*, *Pcdh20*, *C4b*, *AI593442*, and *Gm18517*); at ZT13 (*Slc24a3*, *mt-Nd5*, *Ppp1r3c*, and *C4b*); and at ZT19 (*Aif1l*, *Arrdc2*, *Nes*, *Bcl2l1*, *Piezo1*, *Notch4*, *Cdkn1a*, *Slc2a1*, *Tinagl1*, *Map3k6*, *Errfi1*, *Klf15*, *Tsc22d3*, *Pla2g3*, *Cdh8*, *Dennd3*, *Adgrl4*, *C4b*, *Ehd2*, *Thbd*, *Hspa12b*, and *Gm45461*) (Figures 6B and S6; Table S4). We then checked if these 35 genes were included in the Circadian Expression Profiles Data Browser (CircaDB: http://circadb.hogeneschlab.org/).[26] Of these, 3 of these genes (*Tsc22d3*, *Klf15*, *Aif1l*) were previously characterized as circadian in the brain-related datasets (JTK-q value <0.05), such as those derived from the mouse brainstem, cerebellum, hypothalamus, SCN, and pituitary gland.[27–29]

Furthermore, 24 of these 35 genes lost rhythmicity with age (one-way ANOVA: young $p < 0.05$; aged $p > 0.05$): *Arrdc2*, *Nes*, *Ddah2*, *Bcl2l1*, *Piezo1*, *Notch4*, *Etnppl*, *Cdkn1a*, *Slc2a1*, *Tinagl1*, *Map3k6*, *Errfi1*, *Pla2g3*, *Cdh8*, *Dennd3*, *Adgrl4*, *Pcdh20*, *Slc24a3*, *C4b*, *Ehd2*, *Thbd*, *Hspa12b*, *Gm45461* and *Gm18517* (Figures 6C and S7A). Six genes maintained rhythmicity in both groups but showed changes in their patterns with age (one-way ANOVA: young $p < 0.05$; aged $p < 0.05$, compareRhythms: FDR <0.05): *Aif1l*, *Klf15*, *Tsc22d3*, *Insc*, *Ppp1r3c*, and *AI593442* (Figures 6C and S8A). Five genes gained rhythmicity with age (one-way ANOVA: young $p > 0.05$; aged $p < 0.05$): *Col11a1*, *mt-Nd5*, *Nkain1*, *Gm11611*, and *Rps7-ps3* (Figures 6C and S9A). In particular, some genes such as *Etnppl*, *Tinagl1*, *Hspa12b*, *Ppp1r3c*, *Thbd*, *Pla2g3*, and *Tsc22d3* showed dynamic changes in expression levels between inactive and active periods (i.e., between ZT7 and ZT13, and between ZT1 and ZT19) in young mice (Figure 6D). Finally, we examined these 35 genes using publicly available single-cell RNA-seq data from the adult mouse brain.[30] Several genes such as *Nes*, *Piezo1*, *Notch4*, *Cdkn1a*, *Slc2a1*, *Tinagl1*, *Map3k6*, *Dennd3*, *Adgrl4*, *Ehd2*, *Thbd*, *Hspa12b*, and *Tsc22d3* were predominantly expressed in vascular cells (Figures S7B, S8B, and S9B). On the other hand, *Etnppl* is highly expressed in astrocytes, and *Nkain1* and *Col11a1* are highly expressed in the oligodendrocyte lineage cells (Figures S7B, S8B, and S9B).

DISCUSSION

Our study provides an RNA-seq dataset of the mouse corpus callosum at different ZT and sheds light on the intricate

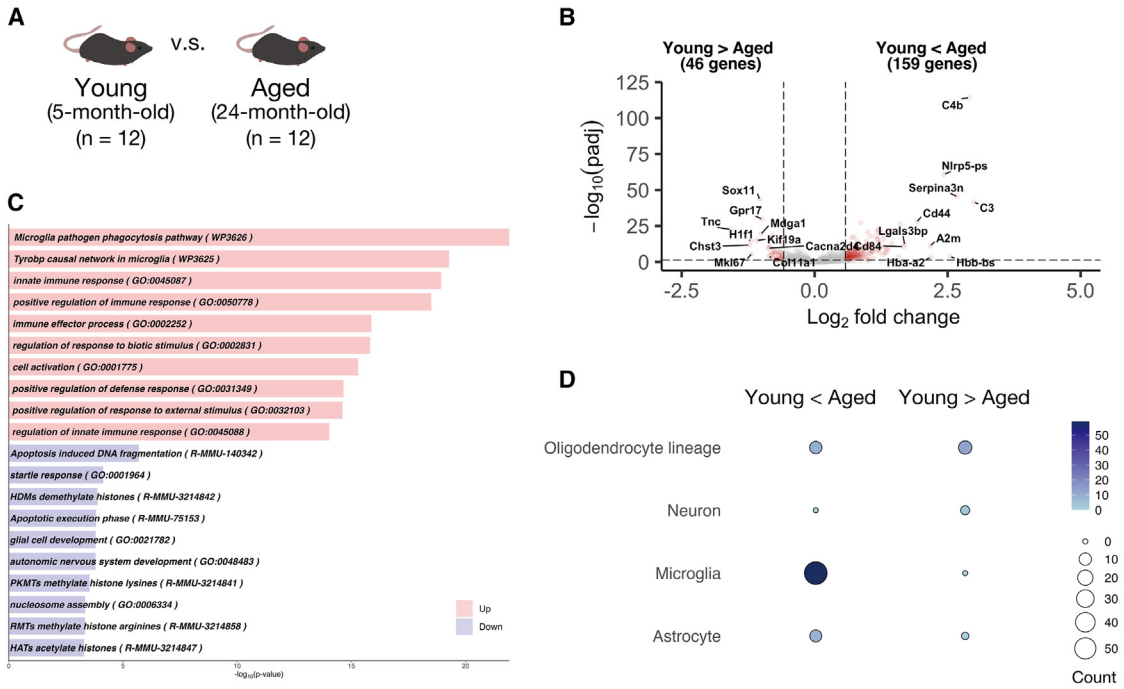

Figure 4. Transcriptomic analysis of the corpus callosum between young and aged mice

(A) Illustration of the groups to detect the DEGs between young and aged mice.

(B) Volcano plot of DEGs (total 205 genes) between young (n = 12; 5 months old) and aged (n = 12; 24 months old) mice. The DEGs cutoff was set at padj <0.05 and | Fold Change | > 1.5.

(C) Top 10 GO terms enriched among genes upregulated (young < aged; red) and downregulated (young > aged; blue) in aged mice.

(D) Classification of the DEGs using cell markers from previously published public RNA-seq data.[24,25]

relationships between diurnal rhythms, aging, and gene expression in a brain region widely considered critical for cognitive function. Our results show that (i) these diurnal differences in gene expression are attenuated in aged vs. young mice, (ii) rhythmically expressed genes are present in white matter and change with aging, and (iii) complement pathways are elevated in aged white matter independent of time of day.

Diurnal and circadian rhythms are regulated by master clock genes. In general, clock genes in aged tissues tend to have dampened oscillation magnitudes and may be slightly phase-shifted compared to young tissues in a wide variety of organs.[31–35] In the brain, age-related disruptions in rhythmicity of *Per1/2*, *Cry1/2*, *Arntl*, and *Clock* were observed in the hypothalamus when comparing 6-month-old versus 26-month-old mice.[31] In the human prefrontal cortex, the rhythmicity of *Per1/2* and *Cry1* was disrupted in the brains of patients greater than 60 years old compared with those under 40 years old.[33] Within the sensitivity limits of our present study, one-way ANOVA analysis did not detect significant differences in the rhythmicity of clock genes in the corpus callosum of 5-month-old versus 24-month-old mice. Furthermore, rhythms were not detected for, *Clock, Cry2*, *Per2*, and *Rora* even in white matter from young mice, in contrast to significant rhythms that have been reported in the hypothalamus.[36] Previous studies have indicated that variations in phase and amplitude of rhythmic clock genes exist across different brain regions.[37–39] For instance, unlike the robust rhythmicity observed in hypothalamic regions, the median septum within white matter and the dentate gyrus of the hippocampus may show arrhythmic patterns.[38] Additionally, a recent work analyzing the human prefrontal cortex in two areas, Brodmann's area 11 (BA11) and BA47, revealed that while *ARNTL* in BA11 showed no impairment in rhythmicity with aging, *ARNTL* in BA47 displayed a significant shift in its rhythmic pattern, indicating that even within the same brain area, different sub-regions might exhibit distinct responses to aging.[33] Recent scRNA-seq analysis now suggests that different cell types within the SCN may exhibit unique temporal patterns of clock genes.[40] Further investigation is needed to examine whether different cell types in mouse white matter may show different clock gene responses to aging.

In addition to light stimulation, fluctuations/oscillations in gene expression are expected to be influenced by factors such as diet and sleep.[41–44] Therefore, although no robust changes in the rhythmicity of key clock genes in the corpus callosum were observed in our study, age-related sleep disruption[45] and/or age-related changes in diet[46–49] and exercise[50] may contribute to age-related changes in gene profiles. Our data that *Etnppl* shows different expression dynamics between young and aged mice would support this idea. *Etnppl* expression increases upon exposure to dexamethasone, an anti-inflammatory drug that binds to the glucocorticoid receptor and is known to be a fasting-induced factor that plays a role in astrocyte lipid homeostasis.[51] A recent large-scale transcriptomic study using mouse striatum during the day suggests that genes with a ZT12

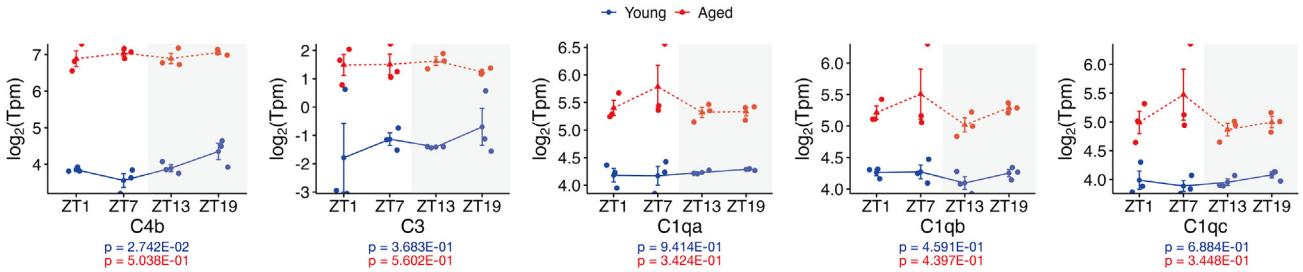

Figure 5. Age-related changes in genes associated with complement activation in the corpus callosum

Line plot illustrating the genes (*C4b*, *C3*, *C1qa*, *C1qb*, and *C1qc*) associated with complement activation in young and aged mice. Data are represented as mean ± SEM. The *p*-values for young mice (blue) and aged mice (red) are derived from one-way ANOVA.

expression peak may be under the control of the adrenocortical hormone glucocorticoid,[52] and in our data, *Etnppl* expression appears to peak between ZT7 and ZT13 in young mice. As perturbations in circulating glucocorticoids and their regulatory hormones have been observed in older humans and aged mice,[53,54] the perturbations in the adrenocortical hormone pathway may influence the observed changes in the expression pattern of *Etnppl*. However, our study is largely descriptive and does not provide the functional validation of the observed gene expression changes. Future experiments using genetic manipulations, pharmacological interventions, or behavioral assays are needed to establish the functional significance of these age-related transcriptomic changes. These studies would elucidate the mechanisms by which age-related changes in sleep and dietary habits affect the transcriptome profile of the mouse corpus callosum.

Our study also suggests an important effect of aging on inflammatory pathways, particularly the complement system, in the corpus callosum. The complement system is a major component of innate immunity and has been implicated in neuroinflammatory processes associated with aging and neurodegeneration.[55–57] For example, C3 is known to exacerbate lipopolysaccharide-induced neuroinflammation,[58] and in our study, C3 was among the top 10 genes that showed age-related increases. C1q was also found to be highly upregulated in the aged corpus callosum in our study. Previous studies show that complement-dependent synaptic pruning by the C1q complex is important during neural development[59] and that uncontrolled complement-mediated synaptic pruning has been reported to be associated with Alzheimer's disease and aging.[60,61] Therefore, the persistent upregulation of complement pathway genes may indicate a chronic inflammatory response or dysregulation associated with aging, which would contribute to age-related cognitive decline and neurodegenerative processes. In addition, Serpina3n functions as a secretory serine protease inhibitor involved in complement activation, and again, *Serpina3n* showed the second highest log2 change between young and aged groups in this study. These changes in the complement system may possibly be due to a gradual breakdown of the blood-brain barrier and are related to general immune activation in the corpus callosum. Interestingly, publicly available transcriptome profiling datasets show that *C4b* and *Seripina3n* are highly expressed in astrocytes and oligodendrocyte lineage cells[30] and that *C4b* is increased in the corpus callosum of aged mice.[62–64] In addition, a recent scRNA-seq dataset using the brains of Alzheimer's disease mice (5xFAD mice) also revealed increased expression of *C4b* and *Serpina3n* in amyloid-beta reactive oligodendrocytes.[65] Although there have been reports that *Serpina3n* was not upregulated in age-related transcriptome data using the mouse hippocampus,[66] our study focused on the corpus callosum (oligodendrocyte-enriched region), which may partly explain the discrepancy.

In summary, this study provides an RNA-seq dataset for understanding the complex interplay between aging, diurnal rhythms, and gene expression within the corpus callosum. By identifying genes influenced by zeitgeber time and characterizing the gene expression changes in aged mice, these findings may provide an important resource for future investigations of how diurnal rhythms and aging intersect to influence cellular processes that mediate neurological health.

Limitations of the study

Our current study provides a valuable resource for investigating the mechanisms by which aging affects the transcriptome profile of the mouse corpus callosum; however, some important caveats/limitations of this study should be noted. First, our findings are based on the analysis of RNA-level data using bulk RNA-seq, which may mask gene expression patterns specific to individual cell types within the corpus callosum due to the averaging of gene expression across different cell populations. In addition, while RNA-seq is a powerful tool for capturing gene expression dynamics, it does not reflect the levels of active and functional proteins within the cell. Therefore, for a more comprehensive understanding of the changes associated with ZT and aging, further investigations incorporating single-cell RNA-seq and proteomics analysis for protein-level validation are warranted. Second, the small sample size and limited number of time points for RNA-seq may affect the reproducibility and generalizability of our analyses. In fact, a recent meta-analysis using publicly available time-series RNA-seq samples of mouse liver tissue highlighted the low reproducibility of circadian transcriptomic studies,[67] suggesting the need for further research with larger sample sizes and additional time points. Nevertheless, the 4-time-point sampling strategy has been successfully used in published studies to draw meaningful conclusions about gene expression rhythms; some studies have even performed RNA-seq analysis at 2 time points to determine time-of-day effects

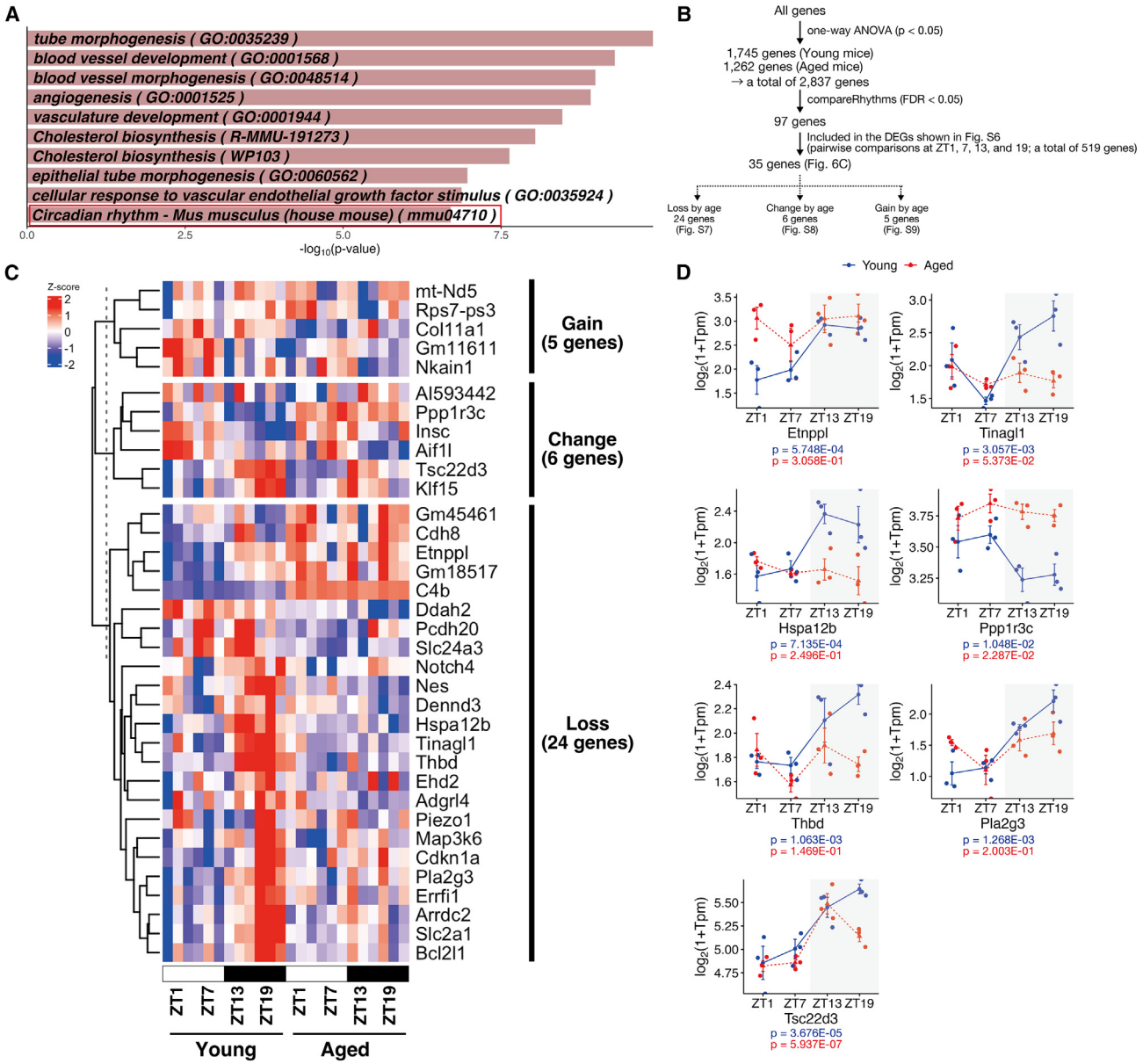

Figure 6. Diurnal rhythm-dependent gene expression in the corpus callosum of young mice and disruption of rhythmicity in aged mice

(A) Bar plots showing the top 10 enriched GO categories for 1,745 genes with diurnal expression patterns in the corpus callosum of young mice identified by one-way ANOVA ($p < 0.05$).

(B) Flowchart summarizing the process of filtering diurnal genes to identify key candidates for further analysis.

(C) Heat maps of 35 genes showing changes in diurnal expression patterns in the corpus callosum between young and aged mice.

(D) Line plots showing the expression levels of *Etnppl*, *Tinagl1*, *Hspa12b*, *Ppp1r3c*, *Thbd*, *Pla2g3*, and *Tsc22d3* at each ZT point in young and aged mice. These genes are a subset of the 35 that exhibited significant changes in diurnal expression patterns between young and aged mice, showing dynamic expression changes between inactive and active periods in young mice. Data are represented as mean ± SEM. The *p*-values for young mice (blue) and aged mice (red) are derived from one-way ANOVA.

on gene expression,[68] and others have used 4 time points to capture diurnal variations.[69–71] These studies demonstrate that significant circadian/diurnal gene expression patterns can be discerned with such sampling schemes. However, while our use of 4 time points is somewhat consistent with established methods in the field, increasing the number of time points to 6 or more would further strengthen our conclusions. Future studies with higher temporal resolution may help to clarify the phase relationships between clock genes and provide a more comprehensive understanding of diurnal gene expression in the aged mouse corpus callosum. Third, it is important to acknowledge that our study focused solely on male mice, which is a limitation.

Investigating sex differences is crucial for a comprehensive understanding of age-related changes in the brain, as there is growing evidence for sexual dimorphism in various aspects of brain aging. Future studies should include both male and female mice to address this important aspect and provide a more complete picture of the aging brain transcriptome. Finally, our data show that the dynamics of these genes in response to ZT are partially lost in aged mice, but this resource article does not directly answer the question of why aging attenuates the diurnal rhythmicity of transcriptome profiles in the mouse corpus callosum. The disruption of normal circadian/diurnal gene expression rhythms in the aged corpus callosum suggests a potential age-related decline in the efficiency of circadian/diurnal regulation. This decline could adversely affect cognitive function and overall brain health, as previous studies have shown that the disruption of circadian/diurnal rhythms can lead to cognitive deficits and neurodegenerative processes. Our data may support the idea that age-related changes in the diurnal transcriptome of the corpus callosum contribute to these pathological processes, but further research is needed to elucidate the specific mechanisms by which altered diurnal gene expression in the aged brain leads to cognitive decline and neurodegeneration. Experiments involving diurnal perturbations in young and aged mice may provide insight into the causal relationship between diurnal rhythms and age-related changes in brain function.

RESOURCE AVAILABILITY

Lead contact

Further information and requests for resources and reagents should be directed to and will be fulfilled by the lead contact, Ken Arai, Ph.D. (karai@partners.org).

Material availability

This study did not generate new unique reagents.

Data and code availability

- The sequence data (FASTQ files) have been deposited at BioProject and are publicly available as of the date of publication. Accession numbers are listed in the key resources table.
- This article does not report the original code.
- Any additional information required to reanalyze the data reported in this article is available from the lead contact upon reasonable request.

ACKNOWLEDGMENTS

We thank our colleagues at the Neuroprotection Research Laboratories, Departments of Radiology and Neurology, Massachusetts General Hospital, and Harvard Medical School. BioRender was used for the graphical abstract. This work was supported by NIH (R01AG081841 to K.A., E.H.L., S.S., and M.E.H.), Alzheimer's Disease Research Foundation (to E.H.L.), Leducq Foundation for Cardiovascular Research (to E.H.L.) and a fellowship from the Uehara Memorial Foundation (to T.H.).

AUTHOR CONTRIBUTIONS

H.I., T.H., E.H.L., and K.A. conceptualized and designed the project. H.I., G.H., E.T.M., and S.G. performed the sample preparation. T.H. and K.A. analyzed the data. T.H. contributed to the visualization and prepared and assembled the figures. H.I., T.H., E.H.L., and K.A. wrote the article. E.H.L. and K.A. provided supervision, project administration, and funding acquisition. G.H., E.T.M., S.G., S.K., N.F., W.L., A.S., S.S., M.E.H., E.H.L., and K.A. provided critical reading and scientific discussions. All authors reviewed and approved the final version of this article.

DECLARATION OF INTERESTS

The authors declare no competing financial interests.

STAR★METHODS

Detailed methods are provided in the online version of this paper and include the following:

- KEY RESOURCES TABLE
- EXPERIMENTAL MODEL AND STUDY PARTICIPANT DETAILS
  - Animals
- METHOD DETAILS
  - Tissue sampling
  - RNA extraction
  - RNA-sequencing
- QUANTIFICATION AND STATISTICAL ANALYSIS

SUPPLEMENTAL INFORMATION

Supplemental information can be found online at https://doi.org/10.1016/j.isci.2024.111556.

Received: March 25, 2024
Revised: June 6, 2024
Accepted: December 5, 2024
Published: December 9, 2024

REFERENCES

1. Hou, Y., Dan, X., Babbar, M., Wei, Y., Hasselbalch, S.G., Croteau, D.L., and Bohr, V.A. (2019). Ageing as a risk factor for neurodegenerative disease. Nat. Rev. Neurol. *15*, 565–581. https://doi.org/10.1038/s41582-019-0244-7.
2. O'Sullivan, M., Jones, D.K., Summers, P.E., Morris, R.G., Williams, S.C., and Markus, H.S. (2001). Evidence for cortical "disconnection" as a mechanism of age-related cognitive decline. Neurology *57*, 632–638. https://doi.org/10.1212/wnl.57.4.632.
3. Andrews-Hanna, J.R., Snyder, A.Z., Vincent, J.L., Lustig, C., Head, D., Raichle, M.E., and Buckner, R.L. (2007). Disruption of Large-Scale Brain Systems in Advanced Aging. Neuron *56*, 924–935. https://doi.org/10.1016/j.neuron.2007.10.038.
4. Mattis, J., and Sehgal, A. (2016). Circadian Rhythms, Sleep, and Disorders of Aging. Trends. Endocrinol. Metab. *27*, 192–203. https://doi.org/10.1016/j.tem.2016.02.003.
5. Musiek, E.S., and Holtzman, D.M. (2016). Mechanisms linking circadian clocks, sleep, and neurodegeneration. Science *354*, 1004–1008. https://doi.org/10.1126/science.aah4968.
6. Esposito, E., Li, W., T. Mandeville, E., Park, J.H., Şencan, I., Guo, S., Shi, J., Lan, J., Lee, J., Hayakawa, K., et al. (2020). Potential circadian effects on translational failure for neuroprotection. Nature *582*, 395–398. https://doi.org/10.1038/s41586-020-2348-z.
7. Takase, H., Hamanaka, G., Hoshino, T., Ohtomo, R., Guo, S., Mandeville, E.T., Lo, E.H., and Arai, K. (2024). Transcriptomic Profiling Reveals Neuroinflammation in the Corpus Callosum of a Transgenic Mouse Model of Alzheimer's Disease. J. Alzheimers. Dis. *97*, 1421–1433. https://doi.org/10.3233/JAD-231049.
8. Skapetze, L., Owino, S., Lo, E.H., Arai, K., Merrow, M., and Harrington, M. (2023). Rhythms in barriers and fluids: Circadian clock regulation in the aging neurovascular unit. Neurobiol. Dis. *181*, 106120. https://doi.org/10.1016/j.nbd.2023.106120.

9. Skapetze, L., Owino, S., Lo, E.H., Arai, K., Merrow, M., and Harrington, M. (2023). Corrigendum to "Rhythms in barriers and fluids: Circadian clock regulation in the aging neurovascular unit". Neurobiol. Dis. *181*, 106162. https://doi.org/10.1016/j.nbd.2023.106162.

10. Kondratov, R.V. (2007). A role of the circadian system and circadian proteins in aging. Ageing. Res. Rev. *6*, 12–27. https://doi.org/10.1016/j.arr.2007.02.003.

11. Kondratova, A.A., and Kondratov, R.V. (2012). The circadian clock and pathology of the ageing brain. Nat. Rev. Neurosci. *13*, 325–335. https://doi.org/10.1038/nrn3208.

12. Zhao, J., Warman, G.R., and Cheeseman, J.F. (2019). The functional changes of the circadian system organization in aging. Ageing Res. Rev. *52*, 64–71. https://doi.org/10.1016/j.arr.2019.04.006.

13. Moore, R.Y., and Eichler, V.B. (1972). Loss of a circadian adrenal corticosterone rhythm following suprachiasmatic lesions in the rat. Brain. Res. *42*, 201–206. https://doi.org/10.1016/0006-8993(72)90054-6.

14. Weaver, D.R. (1998). The suprachiasmatic nucleus: a 25-year retrospective. J. Biol. Rhythms. *13*, 100–112. https://doi.org/10.1177/074873098128999952.

15. Hastings, M.H., Maywood, E.S., and Brancaccio, M. (2018). Generation of circadian rhythms in the suprachiasmatic nucleus. Nat. Rev. Neurosci. *19*, 453–469. https://doi.org/10.1038/s41583-018-0026-z.

16. Stephan, F.K., and Zucker, I. (1972). Circadian rhythms in drinking behavior and locomotor activity of rats are eliminated by hypothalamic lesions. Proc. Natl. Acad. Sci. USA *69*, 1583–1586. https://doi.org/10.1073/pnas.69.6.1583.

17. Brécier, A., Li, V.W., Smith, C.S., Halievski, K., and Ghasemlou, N. (2023). Circadian rhythms and glial cells of the central nervous system. Biol. Rev. Camb. Philos. Soc. *98*, 520–539. https://doi.org/10.1111/brv.12917.

18. Koronowski, K.B., Kinouchi, K., Welz, P.-S., Smith, J.G., Zinna, V.M., Shi, J., Samad, M., Chen, S., Magnan, C.N., Kinchen, J.M., et al. (2019). Defining the Independence of the Liver Circadian Clock. Cellule *177*, 1448–1462.e14. https://doi.org/10.1016/j.cell.2019.04.025.

19. Hor, C.N., Yeung, J., Jan, M., Emmenegger, Y., Hubbard, J., Xenarios, I., Naef, F., and Franken, P. (2019). Sleep-wake-driven and circadian contributions to daily rhythms in gene expression and chromatin accessibility in the murine cortex. Proc. Natl. Acad. Sci. USA *116*, 25773–25783. https://doi.org/10.1073/pnas.1910590116.

20. Zhang, S.L., Lahens, N.F., Yue, Z., Arnold, D.M., Pakstis, P.P., Schwarz, J.E., and Sehgal, A. (2021). A circadian clock regulates efflux by the blood-brain barrier in mice and human cells. Nat. Commun. *12*, 617. https://doi.org/10.1038/s41467-020-20795-9.

21. Bellesi, M., Pfister-Genskow, M., Maret, S., Keles, S., Tononi, G., and Cirelli, C. (2013). Effects of sleep and wake on oligodendrocytes and their precursors. J. Neurosci. *33*, 14288–14300. https://doi.org/10.1523/JNEUROSCI.5102-12.2013.

22. Pelikan, A., Herzel, H., Kramer, A., and Ananthasubramaniam, B. (2022). Venn diagram analysis overestimates the extent of circadian rhythm reprogramming. FEBS J. *289*, 6605–6621. https://doi.org/10.1111/febs.16095.

23. Ananthasubramaniam, B. (2023). bharathananth/compareRhythms: compareRhythms for independently- and longitudinally- sampled time series data. https://doi.org/10.5281/zenodo.7699722.

24. Zhang, Y., Chen, K., Sloan, S.A., Bennett, M.L., Scholze, A.R., O'Keeffe, S., Phatnani, H.P., Guarnieri, P., Caneda, C., Ruderisch, N., et al. (2014). An RNA-Sequencing Transcriptome and Splicing Database of Glia, Neurons, and Vascular Cells of the Cerebral Cortex. J. Neurosci. *34*, 11929–11947. https://doi.org/10.1523/jneurosci.1860-14.2014.

25. Voskuhl, R.R., Itoh, N., Tassoni, A., Matsukawa, M.A., Ren, E., Tse, V., Jang, E., Suen, T.T., and Itoh, Y. (2019). Gene expression in oligodendrocytes during remyelination reveals cholesterol homeostasis as a therapeutic target in multiple sclerosis. Proc. Natl. Acad. Sci. USA *116*, 10130–10139. https://doi.org/10.1073/pnas.1821306116.

26. Pizarro, A., Hayer, K., Lahens, N.F., and Hogenesch, J.B. (2013). CircaDB: A database of mammalian circadian gene expression profiles. Nucleic. Acids. Res. *41*, 1009–1013. https://doi.org/10.1093/nar/gks1161.

27. Panda, S., Antoch, M.P., Miller, B.H., Su, A.I., Schook, A.B., Straume, M., Schultz, P.G., Kay, S.A., Takahashi, J.S., and Hogenesch, J.B. (2002). Coordinated transcription of key pathways in the mouse by the circadian clock. Cell *109*, 307–320. https://doi.org/10.1016/S0092-8674(02)00722-5.

28. Hughes, M.E., DiTacchio, L., Hayes, K.R., Vollmers, C., Pulivarthy, S., Baggs, J.E., Panda, S., and Hogenesch, J.B. (2009). Harmonics of circadian gene transcription in mammals. PLoS Genet. *5*, e1000442. https://doi.org/10.1371/journal.pgen.1000442.

29. Zhang, R., Lahens, N.F., Ballance, H.I., Hughes, M.E., and Hogenesch, J.B. (2014). A circadian gene expression atlas in mammals: Implications for biology and medicine. Proc. Natl. Acad. Sci. USA *111*, 16219–16224. https://doi.org/10.1073/pnas.1408886111.

30. Ximerakis, M., Lipnick, S.L., Innes, B.T., Simmons, S.K., Adiconis, X., Dionne, D., Mayweather, B.A., Nguyen, L., Niziolek, Z., Ozek, C., et al. (2019). Single-cell transcriptomic profiling of the aging mouse brain. Nat. Neurosci. *22*, 1696–1708. https://doi.org/10.1038/s41593-019-0491-3.

31. Wolff, C.A., Gutierrez-Monreal, M.A., Meng, L., Zhang, X., Douma, L.G., Costello, H.M., Douglas, C.M., Ebrahimi, E., Pham, A., Oliveira, A.C., et al. (2023). Defining the age-dependent and tissue-specific circadian transcriptome in male mice. Cell Rep. *42*, 111982. https://doi.org/10.1016/j.celrep.2022.111982.

32. Bonaconsa, M., Malpeli, G., Montaruli, A., Carandente, F., Grassi-Zucconi, G., and Bentivoglio, M. (2014). Differential modulation of clock gene expression in the suprachiasmatic nucleus, liver and heart of aged mice. Exp. Gerontol. *55*, 70–79. https://doi.org/10.1016/j.exger.2014.03.011.

33. Chen, C.Y., Logan, R.W., Ma, T., Lewis, D.A., Tseng, G.C., Sibille, E., and McClung, C.A. (2016). Effects of aging on circadian patterns of gene expression in the human prefrontal cortex. Proc. Natl. Acad. Sci. USA *113*, 206–211. https://doi.org/10.1073/pnas.1508249112.

34. Ando, H., Ushijima, K., Kumazaki, M., Takamura, T., Yokota, N., Saito, T., Irie, S., Kaneko, S., and Fujimura, A. (2010). Influence of age on clock gene expression in peripheral blood cells of healthy women. Journals Gerontol. - Ser. A Biol. Sci. Med. Sci. *65*, 9–13. https://doi.org/10.1093/gerona/glp160.

35. Yamazaki, S., Straume, M., Tei, H., Sakaki, Y., Menaker, M., and Block, G.D. (2002). Effects of aging on central and peripheral mammalian clocks. Proc. Natl. Acad. Sci. USA *99*, 10801–10806. https://doi.org/10.1073/pnas.152318499.

36. Li, W., Wang, Z., Cao, J., Dong, Y., and Chen, Y. (2022). Role of Sleep Restriction in Daily Rhythms of Expression of Hypothalamic Core Clock Genes in Mice. Curr. Issues. Mol. Biol. *44*, 609–625. https://doi.org/10.3390/cimb44020042.

37. Girotti, M., Weinberg, M.S., and Spencer, R.L. (2009). Diurnal expression of functional and clock-related genes throughout the rat HPA axis: System-wide shifts in response to a restricted feeding schedule. Am. J. Physiol. Endocrinol. Metab. *296*, 888–897. https://doi.org/10.1152/ajpendo.90946.2008.

38. Abe, M., Herzog, E.D., Yamazaki, S., Straume, M., Tei, H., Sakaki, Y., Menaker, M., and Block, G.D. (2002). Circadian rhythms in isolated brain regions. J. Neurosci. *22*, 350–356. https://doi.org/10.1523/jneurosci.22-01-00350.2002.

39. Chun, L.E., Woodruff, E.R., Morton, S., Hinds, L.R., and Spencer, R.L. (2015). Variations in phase and amplitude of rhythmic clock gene expression across prefrontal cortex, hippocampus, amygdala, and hypothalamic paraventricular and suprachiasmatic nuclei of male and female rats. J. Biol. Rhythm. *30*, 417–436. https://doi.org/10.1177/0748730415598608.

40. Wen, S., Ma, D., Zhao, M., Xie, L., Wu, Q., Gou, L., Zhu, C., Fan, Y., Wang, H., and Yan, J. (2020). Spatiotemporal single-cell analysis of gene

expression in the mouse suprachiasmatic nucleus. Nat. Neurosci. *23*, 456–467. https://doi.org/10.1038/s41593-020-0586-x.

41. Zhang, Y., and Kutateladze, T.G. (2018). Diet and the epigenome. Nat. Commun. *9*, 3375. https://doi.org/10.1038/s41467-018-05778-1.
42. Gaine, M.E., Chatterjee, S., and Abel, T. (2018). Sleep deprivation and the epigenome. Front. Neural Circ. *12*, 14. https://doi.org/10.3389/fncir.2018.00014.
43. Nam, K.N., Mounier, A., Wolfe, C.M., Fitz, N.F., Carter, A.Y., Castranio, E.L., Kamboh, H.I., Reeves, V.L., Wang, J., Han, X., et al. (2017). Effect of high fat diet on phenotype, brain transcriptome and lipidome in Alzheimer's model mice. Sci. Rep. *7*, 4307–4313. https://doi.org/10.1038/s41598-017-04412-2.
44. Vanrobaeys, Y., Peterson, Z.J., Walsh, E.N., Chatterjee, S., Lin, L.C., Lyons, L.C., Nickl-Jockschat, T., and Abel, T. (2023). Spatial transcriptomics reveals unique gene expression changes in different brain regions after sleep deprivation. Nat. Commun. *14*, 7095–7115. https://doi.org/10.1038/s41467-023-42751-z.
45. Mander, B.A., Winer, J.R., and Walker, M.P. (2017). Sleep and Human Aging. Neuron *94*, 19–36. https://doi.org/10.1016/j.neuron.2017.02.004.
46. Kassis, A., Fichot, M.C., Horcajada, M.N., Horstman, A.M.H., Duncan, P., Bergonzelli, G., Preitner, N., Zimmermann, D., Bosco, N., Vidal, K., and Donato-Capel, L. (2022). Nutritional and lifestyle management of the aging journey: A narrative review. Front. Nutr. *9*, 1087505. https://doi.org/10.3389/fnut.2022.1087505.
47. Leslie, W., and Hankey, C. (2015). Aging, nutritional status and health. Healthcover *3*, 648–658. https://doi.org/10.3390/healthcare3030648.
48. Johnston, R., Poti, J.M., and Popkin, B.M. (2014). Eating and aging: Trends in dietary intake among older Americans from 1977-2010. J. Nutr. Health. Aging. *18*, 234–242. https://doi.org/10.1007/s12603-013-0387-y.
49. Yannakoulia, M., Mamalaki, E., Anastasiou, C.A., Mourtzi, N., Lambrinoudaki, I., and Scarmeas, N. (2018). Eating habits and behaviors of older people: Where are we now and where should we go? Maturitas *114*, 14–21. https://doi.org/10.1016/j.maturitas.2018.05.001.
50. Grevendonk, L., Connell, N.J., McCrum, C., Fealy, C.E., Bilet, L., Bruls, Y.M.H., Mevenkamp, J., Schrauwen-Hinderling, V.B., Jörgensen, J.A., Moonen-Kornips, E., et al. (2021). Impact of aging and exercise on skeletal muscle mitochondrial capacity, energy metabolism, and physical function. Nat. Commun. *12*, 4773. https://doi.org/10.1038/s41467-021-24956-2.
51. White, C.J., Ellis, J.M., and Wolfgang, M.J. (2021). The role of ethanolamine phosphate phospholyase in regulation of astrocyte lipid homeostasis. J. Biol. Chem. *297*, 100830. https://doi.org/10.1016/j.jbc.2021.100830.
52. Wang, N., Langfelder, P., Stricos, M., Ramanathan, L., Richman, J.B., Vaca, R., Plascencia, M., Gu, X., Zhang, S., Tamai, T.K., et al. (2022). Mapping brain gene coexpression in daytime transcriptomes unveils diurnal molecular networks and deciphers perturbation gene signatures. Neuron *110*, 3318–3338.e9. https://doi.org/10.1016/j.neuron.2022.09.028.
53. Boscaro, M., Paoletta, A., Scarpa, E., Barzon, L., Fusaro, P., Fallo, F., and Sonino, N. (1998). Age-related changes in glucocorticoid fats feedback inhibition of adrenocorticotropin in man. J. Clin. Endocrinol. Metab. *83*, 1380–1383. https://doi.org/10.1210/jc.83.4.1380.
54. Valbuena Perez, J.V., Linnenberger, R., Dembek, A., Bruscoli, S., Riccardi, C., Schulz, M.H., Meyer, M.R., Kiemer, A.K., and Hoppstädter, J. (2020). Altered glucocorticoid metabolism represents a feature of macroph-aging. Aging Cell *19*, e13156. https://doi.org/10.1111/acel.13156.
55. Wyss-Coray, T., and Rogers, J. (2012). Inflammation in Alzheimer disease-A brief review of the basic science and clinical literature. Cold Spring Harb. Perspect. Med. *2*, a006346. https://doi.org/10.1101/cshperspect.a006346.
56. Propson, N.E., Gedam, M., and Zheng, H. (2021). Complement in Neurologic Disease. Annu. Rev. Pathol. *16*, 277–298. https://doi.org/10.1146/annurev-pathol-031620-113409.
57. Veerhuis, R., Nielsen, H.M., and Tenner, A.J. (2011). Complement in the brain. Mol. Immunol. *48*, 1592–1603. https://doi.org/10.1016/j.molimm.2011.04.003.
58. Zhou, R., Chen, S.H., Zhao, Z., Tu, D., Song, S., Wang, Y., Wang, Q., Feng, J., and Hong, J.S. (2023). Complement C3 Enhances LPS-Elicited Neuroinflammation and Neurodegeneration Via the Mac1/NOX2 Pathway. Mol. Neurobiol. *60*, 5167–5183. https://doi.org/10.1007/s12035-023-03393-w.
59. Stevens, B., Allen, N.J., Vazquez, L.E., Howell, G.R., Christopherson, K.S., Nouri, N., Micheva, K.D., Mehalow, A.K., Huberman, A.D., Stafford, B., et al. (2007). The Classical Complement Cascade Mediates CNS Synapse Elimination. Cell *131*, 1164–1178. https://doi.org/10.1016/j.cell.2007.10.036.
60. Hong, S., Beja-Glasser, V.F., Nfonoyim, B.M., Frouin, A., Li, S., Ramakrishnan, S., Merry, K.M., Shi, Q., Rosenthal, A., Barres, B.A., et al. (2016). Complement and microglia mediate early synapse loss in Alzheimer mouse models. Science *352*, 712–716. https://doi.org/10.1126/science.aad8373.
61. Shi, Q., Colodner, K.J., Matousek, S.B., Merry, K., Hong, S., Kenison, J.E., Frost, J.L., Le, K.X., Li, S., Dodart, J.C., et al. (2015). Complement C3-deficient mice fail to display age-related hippocampal decline. J. Neurosci. *35*, 13029–13042. https://doi.org/10.1523/JNEUROSCI.1698-15.2015.
62. Allen, W.E., Blosser, T.R., Sullivan, Z.A., Dulac, C., and Zhuang, X. (2023). Molecular and spatial signatures of mouse brain aging at single-cell resolution. Cell *186*, 194–208.e18. https://doi.org/10.1016/j.cell.2022.12.010.
63. Hahn, O., Foltz, A.G., Atkins, M., Kedir, B., Moran-Losada, P., Guldner, I.H., Munson, C., Kern, F., Pálovics, R., Lu, N., et al. (2023). Atlas of the aging mouse brain reveals white matter as vulnerable foci. Cell *186*, 4117–4133.e22. https://doi.org/10.1016/j.cell.2023.07.027.
64. Hoshino, T., Takase, H., Hamanaka, G., Kimura, S., Fukuda, N., Mandeville, E.T., Lok, J., Lo, E.H., and Arai, K. (2024). Transcriptomic changes in oligodendrocyte lineage cells during the juvenile to adult transition in the mouse corpus callosum. Sci. Rep. *14*, 22334. https://doi.org/10.1038/s41598-024-72311-4.
65. Zhou, Y., Song, W.M., Andhey, P.S., Swain, A., Levy, T., Miller, K.R., Poliani, P.L., Cominelli, M., Grover, S., Gilfillan, S., et al. (2020). Human and mouse single-nucleus transcriptomics reveal TREM2-dependent and TREM2-independent cellular responses in Alzheimer's disease. Nat. Med. *26*, 131–142. https://doi.org/10.1038/s41591-019-0695-9.
66. Boehme, M., Guenther, M., Stahr, A., Liebmann, M., Jaenisch, N., Witte, O.W., and Frahm, C. (2014). Impact of indomethacin on neuroinflammation and hippocampal neurogenesis in aged mice. Neurosci. Lett. *572*, 7–12. https://doi.org/10.1016/j.neulet.2014.04.043.
67. Brooks, T.G., Manjrekar, A., Mrčela, A., and Grant, G.R. (2023). Meta-analysis of Diurnal Transcriptomics in Mouse Liver Reveals Low Repeatability of Rhythm Analyses. J. Biol. Rhythm. *38*, 556–570. https://doi.org/10.1177/07487304231179600.
68. Whittaker, D.S., Akhmetova, L., Carlin, D., Romero, H., Welsh, D.K., Colwell, C.S., and Desplats, P. (2023). Circadian modulation by time-restricted feeding rescues brain pathology and improves memory in mouse models of Alzheimer's disease. Cell Metabol. *35*, 1704–1721.e6. https://doi.org/10.1016/j.cmet.2023.07.014.
69. Rojo, D., Dal Cengio, L., Badner, A., Kim, S., Sakai, N., Greene, J., Dierckx, T., Mehl, L.C., Eisinger, E., Ransom, J., et al. (2023). BMAL1 loss in oligodendroglia contributes to abnormal myelination and sleep. Neuron *111*, 3604–3618.e11. https://doi.org/10.1016/j.neuron.2023.08.002.
70. de Assis, L.V.M., Demir, M., and Oster, H. (2023). Nonalcoholic Steatohepatitis Disrupts Diurnal Liver Transcriptome Rhythms in Mice. Cmgh *16*, 341–354. https://doi.org/10.1016/j.jcmgh.2023.05.008.
71. Zhai, Q., Zeng, Y., Gu, Y., Li, Z., Zhang, T., Yuan, B., Wang, T., Yan, J., Qin, H., Yang, L., et al. (2022). Time-restricted feeding entrains long-term behavioral changes through the IGF2-KCC2 pathway. iScience *25*, 104267. https://doi.org/10.1016/j.isci.2022.104267.

72. Dobin, A., Davis, C.A., Schlesinger, F., Drenkow, J., Zaleski, C., Jha, S., Batut, P., Chaisson, M., and Gingeras, T.R. (2013). STAR: Ultrafast universal RNA-seq aligner. Bioinformatics *29*, 15–21. https://doi.org/10.1093/bioinformatics/bts635.

73. Li, B., and Dewey, C.N. (2011). RSEM: accurate transcript quantification from RNA-Seq data with or without a reference genome. BMC. Bioinformatics. *12*, 323. https://doi.org/10.1186/1471-2105-12-323.

74. Love, M.I., Huber, W., and Anders, S. (2014). Moderated estimation of fold change and dispersion for RNA-seq data with DESeq2. Genome. Biol. *15*, 550. https://doi.org/10.1186/s13059-014-0550-8.

75. Zhou, Y., Zhou, B., Pache, L., Chang, M., Khodabakhshi, A.H., Tanaseichuk, O., Benner, C., and Chanda, S.K. (2019). Metascape provides a biologist-oriented resource for the analysis of systems-level datasets. Nat. Commun. *10*, 1523. https://doi.org/10.1038/s41467-019-09234-6.

STAR★METHODS

KEY RESOURCES TABLE

REAGENT or RESOURCE	SOURCE	IDENTIFIER
Chemicals, peptides, and recombinant proteins		
Saline (0.9 w/v% NaCl)	Sigma-Aldrich	Cat#S9625-5KG
Hanks' Balanced Salt Solution (HBSS)	Gibco	Cat#14025-095
QIAzol Lysis Reagent	QIAGEN	Cat#79306
Chloroform Molecular Biology MP Biomedicals	Fisher Scientific	Cat#19400280
Isopropanol (2-Propanol)	Sigma-Aldrich	Cat#190764
RNase-free water	QIAGEN	Cat#129112
Deposited data		
Bulk RNA-seq data derived from young/aged mice (ZT1, ZT7, ZT13, and ZT19)	this paper	PRJNA1011381
Bulk RNA-seq data derived from glia, neurons, and vascular cells of the cerebral cortex	Zhang et al.[24]	GSE52564
Single-cell RNA-seq data from the adult mouse brain	Ximerakis et al.[30]	GSE129788
Experimental models: Organisms/strains		
Male C57BL/6J mice	The Jackson Laboratory	RRID:IMSR_JAX:000664
Software and algorithms		
STAR	Dobin et al.[72]	v2.7.10a RRID:SCR_004463
RSEM	Li et al.[73]	v1.3.3 RRID:SCR_000262
R	R core team	v4.3.0 https://www.r-project.org/ RRID:SCR_001905
DESeq2	Love et al.[74]	v1.40.1 RRID:SCR_015687
compareRhythms	Pelikan et al.[22] and Ananthasubramaniam[23]	v1.0.2
Metascape	Zhou et al.[75]	https://metascape.org/gp/index.html#/main/step1 RRID:SCR_016620

EXPERIMENTAL MODEL AND STUDY PARTICIPANT DETAILS

Animals

All experimental procedures were in accordance with the National Institutes of Health (NIH) guidelines and were approved by the Massachusetts General Hospital Institutional Animal Care and Use Committee. Male C57BL/6J mice were purchased from The Jackson Laboratory and were housed in a specific pathogen-free environment with a 12-h light/dark cycle, with free access to food and water throughout the experiment. During the dark phase, the environment was maintained in complete darkness. However, a brief exposure to dim red light was allowed solely for the purpose of cage retrieval prior to euthanasia at ZT13 and ZT19. In this study, a total of 24 mice (5-month-old, $n = 12$; 24-month-old, $n = 12$) were used. We excluded female mice due to the variable effects of their estrous cycle and the potential for differing age-related changes compared to males, given the longer lifespan of female mice. The sample sizes were determined based on our previous experience and experimental feasibility because this study was conducted based on an exploratory design.

METHOD DETAILS

Tissue sampling

Tissue samples were collected at four different ZTs (ZT1, ZT7, ZT13, and ZT19), with three mice sampled at each time point (Figure 1A). After euthanasia, the mice were perfused with pre-chilled saline followed by decapitation. Before sacrificing the mice at

ZT13 and ZT19, they were briefly exposed to a dim red-light environment and the cages were shaded until just before the sacrifice. Brains were then isolated and cooled in pre-chilled Hanks' Balanced Salt Solution (Gibco, Billings, MT, USA, #14025-095) for 1 min. The brain was sliced into five coronal sections using a brain matrix slicer. To ensure minimal contamination from non-corpus callosum, we carefully isolated the thickest sections of the corpus callosum from the 2nd and 3rd slices. This process was carried out under direct observation using a light microscope. The collected samples were immediately transferred into RNase-free tubes and were frozen in liquid nitrogen.

RNA extraction

Total RNA was extracted from the corpus callosum samples using QIAzol (QIAGEN, Venlo, Netherlands, #79306), according to the manufacturer's instructions. In brief, the tissue was sonicated and then resuspended in 1 mL of pre-chilled QIAzol. Next, 0.2 mL of chloroform was added to the lysate and mixed well using a vortex mixer, followed by centrifugation for 15 min at 12,000 g. The supernatant was then transferred to a new RNase-free tube and mixed with an equal volume of isopropanol. After centrifuging for 10 min at 12,000 g, the pellet was washed with 1 mL of 75% ethanol. The mixture was then centrifuged for 5 min at 7,500 g, and the resultant pellet was resuspended in RNase-free water. The quality and purity of the extracted RNA were determined by NanoDrop Spectrophotometers. The samples were stored at −80°C until further use.

RNA-sequencing

RNA samples from each group were subjected to RNA-seq experiments. Each time point (ZT1, ZT7, ZT13, and ZT19) included three samples (Figure 1A). The library preparation and RNA-seq were handled by MIT BioMicro Center (Cambridge, MA, United States), employing the rRNA depletion method for library preparation (single index) and Illumina NextSeq500 (pair-end; 2 × 150 bp) for RNA-seq sequencing. For data processing, the raw data (FASTQ) was mapped using STAR (version: 2.7.10a; mm10).[72] Transcript abundance was quantified using RSEM (version: 1.3.3).[73] RSEM results included both count data and transcript per kilobase million (TPM) values. Both raw count data and TPM data obtained from the RSEM results are provided in Tables S5 and S6. For most of our analyses, we used the normalized count data. However, for plotting, TPM values were utilized. The bioinformatics analysis was performed using R (version: 4.3.0) and various packages including DESeq2 (version: 1.40.1; Wald test)[74] for differential expression analysis with a cut-off set at an adjusted p-value (padj) < 0.05 for filtering differentially expressed genes (DEGs). Metascape was used for gene ontology (GO) analysis.[75] To investigate rhythmicity, one-way ANOVA was used to assess rhythmic patterns within each group (young and aged) using normalized count data (Table S3). To further assess rhythmic gene expression, we used the compareRhythms (version: 1.0.2)[22,23] to compare diurnal rhythm patterns between young and aged groups. The analysis was performed using normalized count data from DESeq2, with a mean expression threshold of >10 for filtering low-expressed genes. We set the period to 24 h and used the deseq2 method in compareRhythms for RNA-seq analysis. Genes were classified based on their rhythmicity in young and aged mice and whether there was a significant difference in rhythm between the two groups, with a false discovery rate (FDR) < 0.05. Additionally, MESOR (Midline Estimating Statistic of Rhythm) was calculated for each gene using the mean expression at each time point, and genes with a significant difference in MESOR between young and aged groups were identified (adjusted p-value <0.05).

QUANTIFICATION AND STATISTICAL ANALYSIS

All statistical analyses, including one-way and two-way ANOVA, were performed using R. All graphs were generated in R, and error bars in the figures represent the standard error of the mean (SEM). Specific experimental and statistical details are provided in the respective figure legends.